Journal of Materials Chemistry A

PAPER

View Article Online
View Journal | View Issue

Cite this: J. Mater. Chem. A, 2014, 2, 15620

Polythiophenoazomethines – alternate photoactive materials for organic photovoltaics†

Andréanne Bolduc,‡[a] Satyananda Barik,§[a] Martin R. Lenze,[b] Klaus Meerholz*[b] and W. G. Skene*[a]

Received 23rd June 2014
Accepted 24th July 2014

DOI: 10.1039/c4ta03202k

www.rsc.org/MaterialsA

Solution-processable polyazomethines containing thiophenes were synthesized and used as the donor material in bulk heterojunction solar cells. The blue polymers exhibited similar electrochemical properties to the benchmark P3HT with the advantage of absorbing more of the visible spectrum. The resulting photovoltaic devices using polyazomethines in the photoactive layer with $PC_{60}BM$ as the acceptor showed power conversion efficiencies up to 0.22% under simulated 100 mW cm^{-2} AM 1.5G irradiation. The low efficiencies are ascribed to poor charge generation because of too coarse bulk heterojunction morphology formation.

1 Introduction

Conjugated polymers have received much attention as they offer many new possibilities for devices combining unique optical, electrical, and mechanical properties.[1] Of particular interest are their light harvesting and charge transfer properties, especially when combined with electron acceptors such as the fullerene derivative phenyl-C_{61}-butyric acid methyl ester ($PC_{60}BM$). These electron donor–acceptor systems are well suited for uses in organic electronics, especially organic photovoltaic devices (OPVDs).[2]

Much effort has focused on the design and preparation of new polymers for achieving enhanced OPVDs with high power conversion efficiencies (PCE).[3] PCEs up to 9.2% have been achieved by combining different small molecules and donor–acceptor copolymer systems and optimizing the device fabrication including thermal annealing and the use of different cathode materials.[4] Even though research endeavors have concentrated on synthetic optimization, the polymerization of photoactive OPVD materials has exclusively used aryl–aryl coupling reactions including Suzuki,[5] Yamamoto,[6] Grignard metathesis,[7] and C–H activation polymerization protocols.[8] Alternatively, Gilch[9] and Horner–Emmons[10] strategies have also been used for preparing vinylene conjugated polymers. Although these polymerization methods are successful, the preparation of conjugated polymers using these protocols requires rigorous reaction conditions such as catalysts, inert atmospheres and anhydrous solvents.[2d,11] These coupling methods further produce by-products, requiring rigorous product purification for obtaining pristine materials and for ensuring optimal device performance. Interestingly, the PCEs measured for devices prepared from a vast majority of these synthetically demanding materials are below 0.5%.[12] Given the ecological and economic rewards of OPVDs, alternate straightforward coupling methods not requiring stringent protocols and little to no product purification are, therefore, of interest for preparing new photoactive conjugated polymers for use in OPVDs.

Conjugated polymers derived from azomethines (–N=C–) are highly interesting alternatives to conventional coupling protocols in part due to their simple synthesis that does not require the use of stringent reaction conditions or metal catalysts. Polythiophenoazomethine derivatives such as those in Scheme 1 are especially interesting because they have optical and electrochemical properties that are well-suited for use as the light harvesting component in photovoltaic devices.[13] Polyazomethines are also generally interesting because water is the only by-product of the reaction (Scheme 1). As a result,

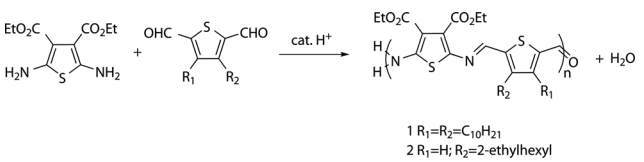

Scheme 1 Acid catalyzed condensation of polyazomethines 1 and 2.

[a]Laboratoire de caractérisation photophysique des matériaux conjugués, Département de Chimie, Pavillon JA Bombardier, Université de Montréal, CP 6128, succ. Centre-ville, Montreal, Quebec, Canada H3T 2B1. E-mail: w.skene@umontreal.ca

[b]Department of Chemistry, University of Cologne, Luxemburger Str. 116, 50939, Cologne, Germany. E-mail: klaus.meerholz@uni-koeln.de

† Electronic supplementary information (ESI) available: NMR, absorbance and FT-IR spectra, GPC elugram, AFM micrographs, and thermograms. See DOI: 10.1039/c4ta03202k

‡ Molecular Science and Technology, Department of Chemical Engineering and Chemistry, Eindhoven University of Technology, Den Dolech 2, 5612 AZ, P.O. Box 513 5600 MB, Eindhoven, The Netherlands.

§ Institute of Chemical and Engineering Sciences, Pesek Road, Jurong Island, 627833, Singapore.

postpolymerization purification of polyazomethines is not required and they can be used as is directly from the polymerization mixture. They can therefore be thought of as green materials with environmental benefits.

Despite the synthetic advantages of conjugated azomethines over currently used polymers in OPVDs, there are only few examples of azomethines used in such devices.[14] These have focused predominately either on small molecules or polymers having limited degrees of conjugation. The latter have narrow absorbance in the visible and limited solubility in solvents used for device preparation. Given the ecological advantages of polyazomethines, we were therefore incited to demonstrate that these easily prepared conjugated polymers consisting uniquely of thiophenes could be used as the photoactive layer in OPVDs, while having key properties for use in such devices, including solution processability and broad absorption in the visible. Herein, we present the polythiophenoazomethines **1** and **2** (Scheme 1) for use in OPVDs as a proof-of-concept to demonstrate that these polyazomethines can be used as materials for photoactive layers in OPVDs.

2 Experimental

2.1 Synthesis

The synthesis of **1** ($M_n = 10$ kg mol^{-1}, $M_w = 15$ kg mol^{-1}, PDI = 1.5, GPC relative to polystyrene standards) was done according to known protocols.[13b,c,15,24] FT-IR: 2925, 2850, 1725, 1670, 1560, 1425, 1220, 1195, 1155, 1095, 1025, 860, 845, 775, 745, 715, 635 cm^{-1}. Anal. Calcd for $C_{36}H_{56}N_2O_5S_2$•11.65 H_2O•0.7 $Sc(OTf)_3$: C 37.65; H 6.58; N 2.30; S 10.82. Found: C 35.86; H 4.77; N 4.01; S 10.71. The synthesis of **2** is given in the following. For NMR spectra as well as TGA, DSC and GPC measurements see ESI.†

3-(2-Ethylhexyl) thiophene. In anhydrous THF (50 mL) was dissolved magnesium (2.65 g, 109 mmol) and 2-ethylhexyl bromide (15 g, 77 mmol) was added. The reaction mixture was stirred for 30 min at 0 °C. The magnesium was allowed to react as much as possible by refluxing the reaction mixture for 2 h to obtain the desired 2-ethylhexyl magnesium bromide. In another flask, 3-bromothiophene (7.0 g, 43 mmol) was dissolved in anhydrous THF (100 mL) to which was then added [1,3-bis (diphenylphosphino) propane] nickel(II) chloride (200 mg, 0.4 mmol). Three cycles of freeze–pump–thaw were performed to ensure complete removal of oxygen. The prepared 2-ethylhexyl magnesium bromide (Grignard reagent) was added to the red coloured solution (second flask) by cannula and the brown solution was then refluxed for 18 h. The solution was washed with aqueous HCl (10% w/w) after cooling to room temperature. The organic phase was extracted with ethyl acetate, dried with $MgSO_4$ filtered, and the solvent was evaporated. The crude product was chromatographed on silica with 100% hexanes to afford a colourless oil (4.9 g, 58%). ^{1}H-NMR ($CDCl_3$): $\delta = 7.26$ (d, 1H), 6.94 (dd, 2H), 2.63 (d, 2H), 1.58 (septet, 1H), 1.32 (m, 8H), 0.91 (dt, 6H). ^{13}C-NMR ($CDCl_3$): $\delta = 142.3$, 129.2, 125.2, 121.0, 40.8, 34.7, 32.9, 29.3, 26.0, 23.5, 14.8, 11.2. HR-MS($^+$) calculated for $[C_{12}H_{20}S + H]^+$: 197.12857; found: 197.12852.

3-(2-Ethylhexyl) thiophene-2,5-dicarbaldehyde. To a solution of 3-(2-ethylhexyl) thiophene (7.5 g, 38 mmol) and freshly distilled TMEDA (9.8 g, 84 mmol) in anhydrous hexanes (50 mL) under nitrogen, was added a solution of 2.0 M *n*-BuLi in hexane (42 mL, 84 mmol) drop-wise. After refluxing for 1.5 h, THF (40 mL) was added and the solution was cooled at −50 °C. Anhydrous DMF (14 mL, 190 mmol) was added drop-wise. After 2.5 h at room temperature, the reaction mixture was hydrolyzed with water (60 mL) and the mixture was extracted with ether. The organic layers were dried over $MgSO_4$ and concentrated. The crude product was purified using column chromatography with hexanes/ethyl acetate (90/10 v/v) to give the product as a colorless oil (7.0 g, 72%). ^{1}H-NMR ($CDCl_3$) δ ppm: 10.13 (s, 1H), 9.98 (s, 1H), 7.63 (s, 1H), 2.92 (d, 2H), 1.61 (septet, 1H), 1.3 (m, 8H), 0.90 (dt, 6H). ^{13}C-NMR ($CDCl_3$): $\delta = 183.8$, 183.4, 151.7, 148.0, 144.3, 138.1, 41.9, 33.1, 32.8, 29.1, 26.0, 23.3, 14.4, 11.1. HR-MS($^+$) calculated for $[C_{14}H_{20}O_2S + H]^+$: 253.12840; found: 253.12842.

Poly(3-(3-octane2-yl)thiophene)-*co*-3,4-diethoxy-thiophenoazomethine (2). The copolymerization was done by mixing 3-(2-ethylhexyl)-thiophene-2,5-dicarbaldehyde (200 mg, 0.79 mmol) and diethyl 2,5-diaminothiophene-3,4-dicarboxylate (204 mg, 0.79 mmol) in $CHCl_3$ (5.0 mL) in a pressure tube. A catalytic amount of diluted TFA (30 μL) was then added. The pressure tube was sealed and heated to 90 °C for 72 h. The reaction mixture was cooled to room temperature and the polymer was precipitated from a methanol–water mixture. The resulting blue solid (85%, 380 mg) was filtered and washed with methanol, water and acetone and then dried under vacuum overnight. In another sample, the solvent was removed under vacuo and the polymer was used as is for subsequent characterization. ^{1}H NMR (400 MHz, $CDCl_3$) δ ppm: 10.13 (m, CHO), 8.52 (m, –N=CH–), 8.07 (s, –Th–H), 4.42 (m, 4H). 2.82 (m, –CH_2), 1.44 (m, –CH–), 1.28 (m, –CH–CH_2–), 0.88 (m, –CH_3). FT-IR: 2955, 2925, 2855, 1720, 1705, 1570, 1535, 1488, 1460, 1420, 1380, 1285, 1245, 1204, 1145, 1095, 1020, 965, 930, 845, 780, 510 cm^{-1}. Anal. calcd for $C_{24}H_{32}N_2O_5S_2$: C 58.61; H 6.55; N 5.69; S 13.02. Found: C 60.59; H 6.46; N 5.93; S 13.66. GPC relative to polystyrene molecular weight standards: $M_n = 10.8$ kg mol^{-1}; $M_w = 15.7$ kg mol^{-1}; PDI = 1.45.

2.2 Spectroscopy and electrochemistry

The spectroscopic properties in solution (dichloromethane) and thin film were measured using a Cary 500 spectrophotometer. The electrochemical properties of the polyazomethines were characterized using a Bio-Logic VSP 300 potentiostat. The compounds were dissolved in deaerated dichloromethane at 10^{-4} M with NBu_4PF_6 (0.5 M). A platinum electrode was used as the working electrode with a platinum wire as the auxiliary electrode. The reference electrode was a saturated Ag/AgCl electrode. Ferrocene was added to the solution as an internal reference ($E_{pa} = 0.35$ V *vs.* Ag/AgCl).[16] The HOMO level of **1** was additionally measured in thin films *via* photoelectron spectroscopy in air with a Riken Keiki AC-2 spectrometer (CSIRO-Clayton, Australia).

2.3 Device fabrication

All devices were fabricated on commercial indium–tin oxide (ITO)-coated glass (Thin Film Devices (TFD), 15 Ω sq^{-1}). The ITO was etched with acid and subsequently cleaned using

chloroform, acetone, Mucasol detergent, and deionized water in an ultrasonic bath. The ITO substrates were next cleaned in an ozone chamber for 10 min. PEDOT : PSS (Clevios P Al 4083, from Heraeus) was then spin coated on the ITO substrates at 3000 rpm for 30 seconds, resulting in 35 nm of the hole-injection layer. Residual water was removed by heat treatment for 2 min at 110 °C. Concentrated stock solutions of equal weight amounts of the corresponding polyazomethine and $PC_{60}BM$ (from Nano-C, Westwood, MA, USA) were individually prepared in chlorobenzene (*ca.* 25 mg mL^{-1}) under inert atmosphere and stirred at room temperature until homogeneous. The solutions were then combined to obtain the desired polyazomethine : $PC_{60}BM$ ratios and then further stirred for four hours. The active layer was deposited by spin coating from solution onto the ITO/PEDOT substrates at different speeds to obtain active layer film thickness ranging between 25 and 80 nm. The bulk heterojunction (BHJ) device was completed by evaporating 4 nm of Ca followed by 110 nm of Ag (99.9%, Alfa Aesar) through a mask, leading to seven solar cells on each substrate, each with an active area of 0.08 cm^2.

2.4 Device characterization

Device characterization was done by measuring the *J–V* characteristics of the solar cells with a Keithley 2425 source-measurement unit. The simulated AM 1.5 light was provided by a filtered Xe lamp. The intensity of 100 mW cm^{-2} of the AM1.5 light was determined using a calibrated inorganic solar cell from the Fraunhofer Institute for Solar Energy (ISE) in Freiburg (Germany) and a reference P3HT : $PC_{60}BM$ cell measured by the same institution. A surface profiler (Dektak, Veeco) was used to determine the active layer thicknesses. UV-vis thin film spectra were taken with a Varian Cary 50 spectrometer.

3 Results and discussion

Despite the synthetic and purification advantages of polyazomethines in addition to their isoelectronic character to C=C homologous polymers, they must have comparable opto-electronic properties to current photoactive OPVD materials in order to be considered as viable alternatives for these materials. For this reason, the opto-electronic properties of **1** and **2** were investigated and compared to the benchmark photoactive material, P3HT.[17] The two polyazomethines were investigated because their different alkylations were expected to lead to different morphologies and hence various device performances, while being soluble in common processing solvents. In particular, desired properties of **1** and **2** are: (i) broad absorption across the visible spectrum for maximum solar spectrum absorption; (ii) hole transport capability; (iii) HOMO and LUMO levels less than −6.1 and −4.1 eV, respectively, for efficient charge transfer between the azomethine and the commonly used electron acceptor $PC_{60}BM$.

Both the photoelectron spectroscopy and the redox properties of **1** were measured for determining the HOMO energy levels. While the photoelectron oxidation was measured from a film of **1** deposited on ITO coated glass in air (Fig. 1), the redox values of both **1** and **2** were measured in solution by cyclic voltammetry (inset Fig. 1). The advantage of the photoelectron oxidation method is that the HOMO level can directly be measured without relying on the electrochemical oxidation onset.[18] The measured HOMO by the photoelectron oxidation method is consistent with the HOMO derived from the oxidation onset according to the commonly accepted approximation: HOMO = $-e(E_{pa}^{onset}$ (**1** or **2**) + 4.72), where the potentials are measured against Ag/Ag^+,[19] by taking the E_o' of ferrocene that was used as the internal reference to be 0.35 V *vs.* Ag/AgCl.[20] The reduction potential measured by cyclic voltammetry can equally be used to calculate the LUMO level according to: LUMO = $-e(E_{pc}^{onset}$ (**1** or **2**) + 4.72).

The energy-gap (E_g) can further be calculated from either the solution electrochemical data or thin film absorbance onset. Upon comparing the measured data summarized in Table 1 for the azomethines **1** and **2** to P3HT, it is apparent that the HOMO levels of the azomethines are slightly lower than that of P3HT. However, the LUMO levels of the polyazomethines are higher than the LUMO level of $PC_{60}BM$. Although the energy offset between $PC_{60}BM$ and the azomethines is small, charge injection into the electron accepting material from the excited azomethines is nonetheless expected.

The absorbance spectra of **1** relative to P3HT is displayed in Fig. 2. From this figure, it can be seen that the polyazomethine absorbs at 625 nm, *ca.* 200 nm bathochromically shifted relative to P3HT. The observed spectroscopic redshift is a result of the high degree of conjugation concomitant with intramolecular charge transfer effects of the imine/esters of the polyazomethines. Similar absorbance was also seen with **2** (Fig. 2). The absorbance maximum at 625 nm as well as the absorbance onset were found not to shift with concentration (see Fig. S9 in the ESI†). This confirms that the absorbance is insensitive to intermolecular effects. Also, the polyazomethines intrinsically absorb more of the visible spectrum than P3HT. Meanwhile, the similar spectral properties of both **1** and **2** in solution and thin

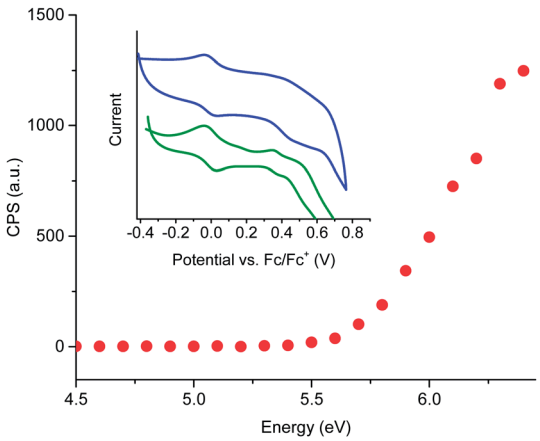

Fig. 1 Photoelectron oxidation of **1** cast as a thin film on an ITO coated glass slide. Inset: cyclic voltammograms of **1** (—) and **2** (—) in dichloromethane measured at 100 mV s^{-1} with $TBAPF_6$ against ferrocene/ferrocenium in anhydrous dichloromethane with ferrocene added as an internal reference.

Table 1 Comparative HOMO, LUMO and band gap energy values of donors and $PC_{60}BM$

Compound	HOMO	LUMO	E_g[b] (eV)
1	−5.5 (−5.6)[a]	−3.9	1.6 (1.6)
2	−5.5	−4.0	1.5 (1.6)
P3HT[c]	−5.1 (−4.8)	−2.7	2.0 (1.9)
$PC_{60}BM$[d]	−6.1	−4.1	2.0

[a] Value in parentheses is from photoelectron spectroscopy. [b] Value in parentheses is the spectroscopically derived energy-gap from the absorbance onset. [c] From literature measured in solution. Value in parentheses is measured in the solid state for P3HT.[21] [d] From literature.[22]

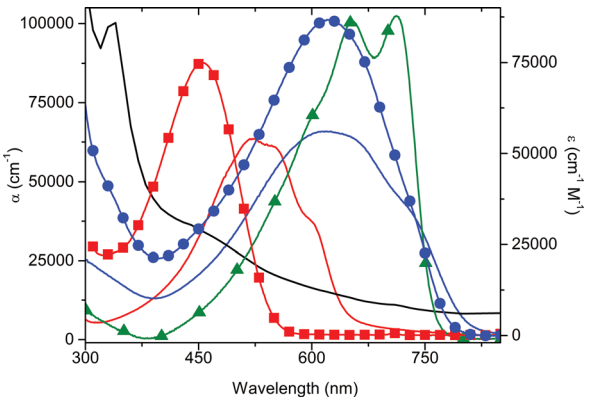

Fig. 2 Absorbance spectra of **1** (●) and **2** (▲) in solution, **1** in thin films measured on glass slides (—), P3HT in solution (■) and in thin films (—), as well as $PC_{60}BM$ (—).

films provide sound evidence that the length of the pendant solubilizing alkyl groups does not affect the optical properties. No spectral shifts were seen with either **1** or **2** upon annealing after spin coating onto glass slides. This is in contrast to P3HT that shifts to longer wavelengths upon annealing because of increased ordering of the polymer chains and formation of aggregated domains.[23]

Discrete repeating patterns associated with highly ordered crystalline materials were previously found to be absent in the powder X-ray diffraction (XRD) of **1**.[24] Instead, the powder XRD was consistent with limited intermolecular π-stacking with a separation distance of 23 Å between the polymer backbones. This large separation is in part a result of interdigitation of the C10-alkyl chains. To further examine the intermolecular packing and self-assembly behavior of **1**, the polymer was spin coated onto silica substrates from solutions of different concentrations and the resulting morphologies were measured by atomic force microscopy (AFM). As seen in Fig. 3, an unordered (amorphous) morphology is adopted at low concentrations (0.5 mg mL^{-1}). In contrast, an organized herringbone-like morphology is received at high concentrations (2 mg mL^{-1}), while small domains occur at intermediate concentrations. The self-organization at higher concentrations is a result of interdigitation of the C10 alkyl chains, which is consistent with the powder XRD data.

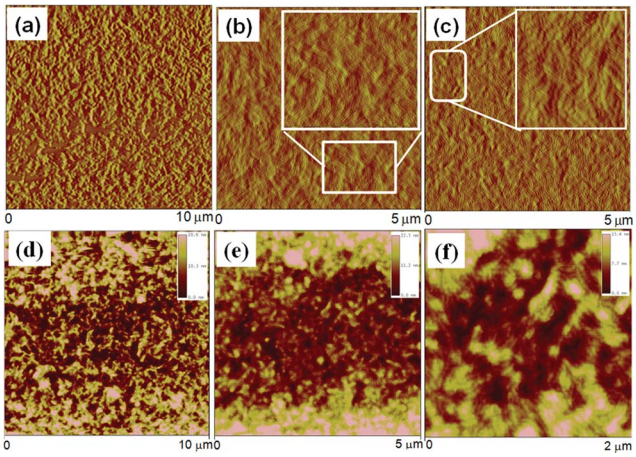

Fig. 3 AFM phase images of **1** showing the different morphologies formed on silica substrates at different concentrations; (a) 0.5 mg mL^{-1}, (b) 1.0 mg mL^{-1} and (c) 2.0 mg mL^{-1} in chloroform and their corresponding topography images (d)–(f).

Bulk-heterojunction OPVDs were fabricated with the polyazomethines using an optimized polymer/acceptor ratio of 1 : 4 and an active layer film thickness of 80 nm (see Fig. S15 and S16 in the ESI†). The devices were fabricated using the conventional ITO/PEDOT : PSS (35 nm)/polyazomethine : $PC_{60}BM$ (80 nm)/Ca (4 nm)/Ag (120 nm) device architecture under anaerobic conditions. Illumination of the devices with simulated AM1.5 (100 mW cm^{-2}) gave the *J*–*V* response reported in Fig. 4. The averaged device characteristics of the investigated solar cells are summarized in Table 2.

There was no change in device performance when using either purified or as-prepared **1**. A *J*–*V* response could not be measured with a device fabricated without **1** or **2**, *i.e.* pure $PC_{60}BM$ as active layer, confirming that the polyazomethine indeed harvests photons and undergoes photoinduced electron transfer with $PC_{60}BM$.

The theoretical maximum V_{oc} of an OPVD can be derived from the energy difference between the HOMO energy levels of

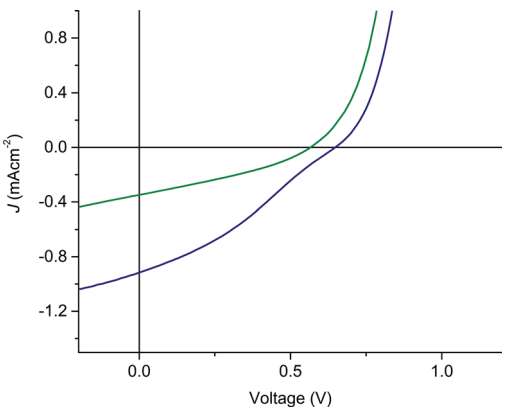

Fig. 4 Representative *J*–*V* response of photovoltaic devices prepared of **1** : $PC_{60}BM$ (1 : 4) (—) and **2** : $PC_{60}BM$ (1 : 4) (—) under simulated AM1.5 illumination of 100 mW cm^{-2} intensity.

Table 2 Representative solar cell characteristics of the investigated OPVDs under simulated AM1.5 illumination of 100 mW cm^{-2}

Compound	V_{oc}/V	J_{SC}/mA cm^{-2}	FF	%PCE
1 : $PC_{60}BM$	0.65	0.94	0.32	0.22
2 : $PC_{60}BM$	0.56	0.37	0.34	0.07
P3HT : $PC_{60}BM$	0.67	8.40	0.53	2.83

the polyazomethines and the LUMO of $PC_{60}BM$ and is equal to *ca.* 1.4 V.[25] The discrepancy between the experimental and theoretical V_{oc} is comparable to most reported photoactive materials, including our reference device prepared from P3HT.[26] This can be attributed to intramolecular charge transfer of the donor and acceptors.[27]

In contrast to the V_{oc}, the fill factor (FF) is lower than in devices prepared with conventional polymers. The low fill factor most likely results from poor hole mobility in the photoactive layer. This is confirmed by field effect transistor measurements of **1** that showed hole mobilities on the order of 10^{-8} cm^2 V^{-1} s^{-1}.[24] This is in contrast to the oligomeric analogue of **1** whose mobilities are on the order of 10^{-5} cm^2 V^{-1} s^{-1}.[24] The increased small molecular ordering in part results in a higher short-circuit current density (J_{SC} = 3.7 mA cm^{-2}), and in turn, a larger PCE ≈ 1.1%.[14a] The measured low mobilities of **1** are therefore not representative of poor intrinsic mobility properties of the polymer, but rather result from limited π-stacking of the thiophene units, which is required for efficient interchain hopping.

The measured short-circuit current density (J_{SC}) for the BHJ devices is considerably smaller than that of P3HT : $PC_{60}BM$. In general, low J_{SC} values can be attributed to two main reasons: (i) no photoinduced charge is produced due to coarse phase separation of the donor and acceptor domains in the BHJ, *i.e.* excitons do not reach the D/A interface within their lifetime (ii) generated charges do not reach the electrode interface due to the absence of continuous percolation pathways and/or high degree of recombination.

Interestingly, AFM phase measurements (Fig. 5a) of the device did not show a uniform morphology expected for a BHJ. Instead, tightly packed grains of $PC_{60}BM$ measuring *ca.* 300 nm in diameter were found. Histogram analysis of the phase image indicates an almost complete separation into the pristine donor and acceptor phases (Fig. 5b). The data could be fitted with two distributions, assigned to polyazomethine-rich ($PC_{60}BM$-poor) and $PC_{60}BM$-rich (azomethine-poor) phases, yielding an area ratio of 1 : 2.5. This morphology does not promote efficient exciton dissociation into free charge carriers. Therefore, the low photocurrent of **1** in blends with $PC_{60}BM$ is most likely the result of poor charge generation. Favorable coarse 20 nm domain size for efficient charge generation while maintaining continuous percolation pathways to the electrodes is expected by varying the length of the alkyl chains. It was originally expected that **2** would exhibit better device performance because of its mono alkylation that would favor smaller domain sizes. However, since no increase in the device performance was observed for **2** (see Table 2), additional modifications besides

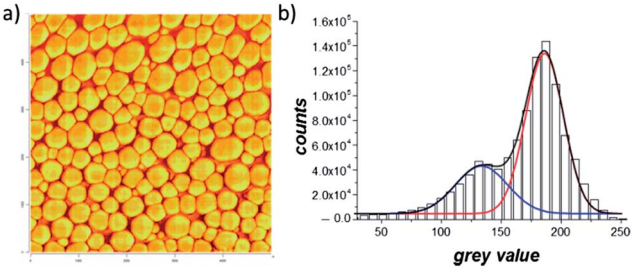

Fig. 5 (a) AFM phase image of 5 × 5 μm area for a 1 : 4 PVD of **1** : $PC_{60}BM$ device and (b) histogram analysis of the phase signal with Gaussian fits: polyazomethine-rich phase (blue) and PCBM-rich phase (red). For AFM topography see Fig. S17 in the ESI.†

alkyl substitution as well as optimization of the OPVD processing conditions are required for improved device efficiencies. Nonetheless, the collective opto-electronic device measurements confirm that the polyazomethines have inherent opto-electronic properties that are suitable for use as a photoactive material in photovoltaics. Increased device efficiencies are expected by modifying the polymer to promote the formation of a more favorable BHJ morphology.

4 Conclusions

In summary, a photovoltaic device using an all-thiophene conjugated polyazomethine as the photoactive layer was demonstrated. It was shown that the V_{oc} of the device was comparable to photoactive materials currently used (≈0.7 V). A small fill factor (<0.35) was measured, which could be attributed to the low hole mobility that results from poor π-staking of the thiophene repeating units.

Although the device PCE is not in the top performance bracket, it nonetheless serves to illustrate that polyazomethines can be used as photoactive and electron donor materials. In fact, the measured performance is comparable to many conjugated polymers examined in photovoltaic devices and whose synthesis is not straightforward, requiring multiple steps and extensive purification. Taking into account the similar properties compared to many of its carbon counterparts together with the ease of synthesis and no purification required for their synthesis, polyazomethines are attractive alternatives for photoactive materials. With additional material optimization including shorter alkyl chains and different donor–acceptor repeating units, improved device efficiencies are expected for polyazomethine based OPVDs.

Acknowledgements

The authors acknowledge financial support from the Natural Sciences and Engineering Research Council Canada for both a DG and SRG in addition to the Centre for Self-Assembled Chemical Structures and additional equipment funding from the Canada Foundation for Innovation. Appreciation is also extended to NanoQuébec. WGS also thanks the Alexander von Humboldt Foundation for fostering this collaborative research

and the RSC for the JWT Jones Travelling Fellowship and CSIRO for photoelectron spectrometer access. AB thanks NSERC, Fonds de recherche Nature et technologies Québec (FQRNT), and the Université de Montréal for graduate scholarships. AB also acknowledges FQRNT for a mobility grant. We thank Dr Jörg-Bernd Bonekamp for analysis of the AFM images. Ms. Zahra Awan is thanked for assistance with FT-IR measurements.

Notes and references

1 (*a*) C. D. Dimitrakopoulos and P. R. L. Malenfant, *Adv. Mater.*, 2002, **14**, 99–117; (*b*) L. Rupprecht, *Conductive Polymers and Plastics in Industrial Applications*, Society of Plastics Engineers/Plastics Design Library, Brookfield, Conn., 1999.

2 (*a*) F. C. Krebs, N. Espinosa, M. Hösel, R. R. Søndergaard and M. Jørgensen, *Adv. Mater.*, 2014, **26**, 29–39; (*b*) A. J. Heeger, *Adv. Mater.*, 2014, **26**, 10–28; (*c*) M. T. Dang, L. Hirsch, G. Wantz and J. D. Wuest, *Chem. Rev.*, 2013, **113**, 3734–3765; (*d*) N. Blouin and M. Leclerc, *Acc. Chem. Res.*, 2008, **41**, 1110–1119.

3 S. A. Jenekhe, *Chem. Mater.*, 2004, **16**, 4381–4382.

4 (*a*) Z. He, C. Zhong, S. Su, M. Xu, H. Wu and Y. Cao, *Nat. Photonics*, 2012, **6**, 591–595; (*b*) A. K. K. Kyaw, D. H. Wang, D. Wynands, J. Zhang, T.-Q. Nguyen, G. C. Bazan and A. J. Heeger, *Nano Lett.*, 2013, **13**, 3796–3801.

5 J. Sakamoto, M. Rehahn, G. Wegner and A. D. Schlüter, *Macromol. Rapid Commun.*, 2009, **30**, 653–687.

6 (*a*) T. Yamamoto, M. Usui, H. Ootsuka, T. Iijima, H. Fukumoto, Y. Sakai, S. Aramaki, H. M. Yamamoto, T. Yagi, H. Tajima, T. Okada, T. Fukuda, A. Emoto, H. Ushijima, M. Hasegawa and H. Ohtsu, *Macromol. Chem. Phys.*, 2010, **211**, 2138–2147; (*b*) E. Scheler and P. Strohriegl, *Chem. Mater.*, 2010, **22**, 1410–1419.

7 (*a*) K. Takagi, H. Joo, Y. Yamashita, E. Kawagita and C. Torii, *J. Polym. Sci., Part A: Polym. Chem.*, 2011, **49**, 4013–4020; (*b*) L. Zhang, K. Tajima and K. Hashimoto, *Macromolecules*, 2011, **44**, 4222–4229.

8 C.-Y. He, C.-Z. Wu, Y.-L. Zhu and X. Zhang, *Chem. Sci.*, 2014, **5**, 1317–1321.

9 (*a*) M. Song, J. S. Park, K. J. Yoon, C.-H. Kim, M. J. Im, J. S. Kim, Y.-S. Gal, J. W. Lee, J. H. Lee and S.-H. Jin, *Org. Electron.*, 2010, **11**, 969–978; (*b*) B. J. Laughlin and R. C. Smith, *Macromolecules*, 2010, **43**, 3744–3749.

10 C. Zhang, T. Matos, R. Li, S.-S. Sun, J. E. Lewis, J. Zhang and X. Jiang, *Polym. Chem.*, 2010, **1**, 663–669.

11 (*a*) N. Yu, R. Zhu, B. Peng, W. Huang and W. Wei, *J. Appl. Polym. Sci.*, 2008, **108**, 2438–2445; (*b*) J.-F. Morin, N. Drolet, Y. Tao and M. Leclerc, *Chem. Mater.*, 2004, **16**, 4619–4626; (*c*) P.-L. T. Boudreault, A. Najari and M. Leclerc, *Chem. Mater.*, 2010, **23**, 456–469; (*d*) P.-L. T. Boudreault, S. Beaupre and M. Leclerc, *Polym. Chem.*, 2010, **1**, 127–136.

12 (*a*) J. Zhou, X. Wan, Y. Liu, F. Wang, G. Long, C. Li and Y. Chen, *Macromol. Chem. Phys.*, 2011, **212**, 1109–1114; (*b*) Z. G. Zhang, H. J. Fan, J. Min, S. Y. Zhang, J. Zhang, M. J. Zhang, X. Guo, X. W. Zhan and Y. F. Li, *Polym. Chem.*, 2011, **2**, 1678–1687; (*c*) W. Zhang, G. M. Ng, H. L. Tam, M. S. Wong and F. Zhu, *J. Polym. Sci., Part A: Polym. Chem.*, 2011, **49**, 1865–1873; (*d*) Q. Wang and W.-Y. Wong, *Polym. Chem.*, 2011, **2**, 432–440; (*e*) J. R. Moore, S. Albert-Seifried, A. Rao, S. Massip, B. Watts, D. J. Morgan, R. H. Friend, C. R. McNeill and H. Sirringhaus, *Adv. Energy Mater.*, 2011, **1**, 230–240; (*f*) J. F. Mike, K. Nalwa, A. J. Makowski, D. Putnam, A. L. Tomlinson, S. Chaudhary and M. Jeffries-El, *Phys. Chem. Chem. Phys.*, 2011, **13**, 1338–1344; (*g*) J. Mei, K. R. Graham, R. Stalder, S. P. Tiwari, H. Cheun, J. Shim, M. Yoshio, C. Nuckolls, B. Kippelen, R. K. Castellano and J. R. Reynolds, *Chem. Mater.*, 2011, **23**, 2285–2288; (*h*) K. A. Mazzio, M. Yuan, K. Okamoto and C. K. Luscombe, *ACS Appl. Mater. Interfaces*, 2011, **3**, 271–278; (*i*) Y.-J. Cheng, L.-C. Hung, F.-Y. Cao, W.-S. Kao, C.-Y. Chang and C.-S. Hsu, *J. Polym. Sci., Part A: Polym. Chem.*, 2011, **49**, 1791–1801; (*j*) M. Helgesen, M. Bjerring, N. C. Nielsen and F. C. Krebs, *Chem. Mater.*, 2010, **22**, 5617–5624; (*k*) X. Guo, H. Xin, F. S. Kim, A. D. T. Liyanage, S. A. Jenekhe and M. D. Watson, *Macromolecules*, 2010, **44**, 269–277; (*l*) H. Diliën, A. Palmaerts, M. Lenes, B. de Boer, P. Blom, T. J. Cleij, L. Lutsen and D. Vanderzande, *Macromolecules*, 2010, **43**, 10231–10240; (*m*) S. Wen, J. Pei, Y. Zhou, P. Li, L. Xue, Y. Li, B. Xu and W. Tian, *Macromolecules*, 2009, **42**, 4977–4984; (*n*) C.-H. Chen, C.-H. Hsieh, M. Dubosc, Y.-J. Cheng and C.-S. Hsu, *Macromolecules*, 2009, **43**, 697–708; (*o*) D. J. Lipomi, R. C. Chiechi, W. F. Reus and G. M. Whitesides, *Adv. Funct. Mater.*, 2008, **18**, 3469–3477; (*p*) S. Rajaram, P. B. Armstrong, B. J. Kim and J. M. J. Fréchet, *Chem. Mater.*, 2009, **21**, 1775–1777.

13 (*a*) S. Barik and W. G. Skene, *Polym. Chem.*, 2011, **2**, 1091–1097; (*b*) S. Barik and W. G. Skene, *Macromolecules*, 2010, **43**, 10435–10441; (*c*) M. Bourgeaux and W. G. Skene, *Macromolecules*, 2007, **40**, 1792–1795.

14 (*a*) M. Petrus, R. Bouwer, U. Lafont, S. Athanasopoulos, N. C. Greenham and T. J. Dingemans, *J. Mater. Chem. A*, 2014, **2**, 9474–9477; (*b*) A. Iwan, B. Boharewicz, I. Tazbir, A. Sikora, E. Schab-Balcerzak, M. Grucela-Zajac and Ł. Skorka, *Synth. Met.*, 2014, **189**, 183–192; (*c*) M. L. Petrus, R. K. M. Bouwer, U. Lafont, D. H. K. Murthy, R. J. P. Kist, M. L. Bohm, Y. Olivier, T. J. Savenije, L. D. A. Siebbeles, N. C. Greenham and T. J. Dingemans, *Polym. Chem.*, 2013, **4**, 4182–4191; (*d*) M. Palewicz, A. Iwan, M. Sibinski, A. Sikora and B. Mazurek, *Energy Procedia*, 2011, **3**, 84–91; (*e*) A. Iwan, M. Palewicz, M. Krompiec, M. Grucela-Zajac, E. Schab-Balcerzak and A. Sikora, *Spectrochim. Acta, Part A*, 2012, **97**, 546–555; (*f*) A. Iwan, M. Palewicz, A. Chuchmała, L. Gorecki, A. Sikora, B. Mazurek and G. Pasciak, *Synth. Met.*, 2012, **162**, 143–153; (*g*) C. O. Sánchez, J. C. Bèrnede, L. Cattin, M. Makha and N. Gatica, *Thin Solid Films*, DOI: 10.1016/j.tsf.2014.04.071.; (*h*) J. C. Hindson, B. Ulgut, R. H. Friend, N. C. Greenham, B. Norder, A. Kotlewski and T. J. Dingemans, *J. Mater. Chem.*, 2010, **20**, 937–944; (*i*) A. Iwan, E. Schab-Balcerzak, D. Pociecha, M. Krompiec, M. Grucela, P. Bilski, M. Kłosowski and H. Janeczek, *Opt. Mater.*, 2011, **34**, 61–74; (*j*) A. Iwan, M. Palewicz, A. Chuchmała, A. Sikora, L. Gorecki and D. Sek, *High*

Perform. Polym., 2013, **25**, 832–842; (*k*) A. Iwan, E. Schab-Balcerzak, K. P. Korona, S. Grankowska and M. Kamińska, *Synth. Met.*, 2013, **185–186**, 17–24; (*l*) G. D. Sharma, S. G. Sandogaker and M. S. Roy, *Thin Solid Films*, 1996, **278**, 129–134.

15 A. Bolduc and W. G. Skene, *Polym. Chem.*, 2014, **5**, 1119–1123.

16 N. Tsierkezos, *J. Solution Chem.*, 2007, **36**, 289–302.

17 H. Ma, H.-L. Yip, F. Huang and A. K. Y. Jen, *Adv. Funct. Mater.*, 2010, **20**, 1371–1388.

18 R. J. Davis, M. T. Lloyd, S. R. Ferreira, M. J. Bruzek, S. E. Watkins, L. Lindell, P. Sehati, M. Fahlman, J. E. Anthony and J. W. P. Hsu, *J. Mater. Chem.*, 2011, **21**, 1721–1729.

19 (*a*) J. Pommerehne, H. Vestweber, W. Guss, R. F. Mahrt, H. Bässler, M. Porsch and J. Daub, *Adv. Mater.*, 1995, **7**, 551–554; (*b*) H. M. Koepp, H. Wendt and H. Stkehlow, *Z. Elektrochem.*, 1960, **64**, 483–491; (*c*) Q. Sun, H. Wang, C. Yang and Y. Li, *J. Mater. Chem.*, 2003, **13**, 800–806; (*d*) Y. Lu, Z. Xiao, Y. Yuan, H. Wu, Z. An, Y. Hou, C. Gao and J. Huang, *J. Mater. Chem. C*, 2013, **1**, 630–637.

20 N. G. Connelly and W. E. Geiger, *Chem. Rev.*, 1996, **96**, 877–910.

21 L. J. A. Koster, V. D. Mihailetchi and P. W. M. Blom, *Appl. Phys. Lett.*, 2006, **88**, 093511.

22 M. Al-Ibrahim, H. K. Roth, U. Zhokhavets, G. Gobsch and S. Sensfuss, *Sol. Energy Mater. Sol. Cells*, 2005, **85**, 13–20.

23 V. Shrotriya, J. Ouyang, R. J. Tseng, G. Li and Y. Yang, *Chem. Phys. Lett.*, 2005, **411**, 138–143.

24 D. Işık, C. Santato, S. Barik and W. G. Skene, *Org. Electron.*, 2012, **13**, 3022–3031.

25 M. C. Scharber, D. Mühlbacher, M. Koppe, P. Denk, C. Waldauf, A. J. Heeger and C. J. Brabec, *Adv. Mater.*, 2006, **18**, 789–794.

26 Y. He, C. Chen, E. Richard, L. Dou, Y. Wu, G. Li and Y. Yang, *J. Mater. Chem.*, 2012, **22**, 13391–13394.

27 (*a*) D. Veldman, S. C. J. Meskers and R. A. J. Janssen, *Adv. Funct. Mater.*, 2009, **19**, 1939–1948; (*b*) D. Di Nuzzo, G.-J. A. H. Wetzelaer, R. K. M. Bouwer, V. S. Gevaerts, S. C. J. Meskers, J. C. Hummelen, P. W. M. Blom and R. A. J. Janssen, *Adv. Energy Mater.*, 2013, **3**, 85–94.